Intracavity second-harmonic generation: The steady-state solutions

A. G. Vladimirov
Physics Faculty, St. Petersburg State University, Ulianovskaya Street 1, 198904 St. Petersburg, Russia

Paul Mandel
Optique Nonlinéaire Théorique, Campus Plaine Code Postal 231, Université Libre de Bruxelles, B-1050 Bruxelles, Belgium

(Received 28 April 1998)

We study the steady states of a solid-state laser containing a birefringent frequency-doubling crystal such as a YAG-KTP laser and assess their stability in a systematic way. We show that as the pump power is increased, different scenarios arise: Hopf bifurcation to antiphased periodic regimes, mode hopping between different cw states, and finally breakup of the multimode states for a single- or two-mode cw regime involving homoclinic points. [S1050-2947(98)07610-0]

PACS number(s): 42.65.Sf, 42.60.Mi, 42.55.Rz

I. INTRODUCTION

Diode-pumped solid-state lasers with intracavity frequency-doubling crystal have proved to be efficient sources of visible light. Therefore the problem of output intensity stability is very important for these lasers. It was shown theoretically and experimentally that when increasing the nonlinear coupling between the modes, the frequency-doubled laser can start to exhibit large amplitude oscillations of modal intensities [1] due to sum-frequency generation. These oscillations are undesirable in many applications since they lead to a laser output with an intensity fluctuating in time (the so-called green problem). On the other hand, antiphase oscillations were shown to exhibit very peculiar properties [2–5] that also could have some applications [6].

Most theoretical works on the antiphase oscillations were devoted to their numerical study and analytical description of their onset associated with degenerate Hopf bifurcations. In [3,5,7,8] the stability of the steady-state solutions was analyzed for a model of frequency-doubled laser. In particular, a complete stability analysis of the two-mode laser is given in [7]. It was shown that the stable steady-state solution corresponding to the N-mode regime for which all the modes in a given polarization have nonzero and equal intensities can exhibit both Hopf and steady-state bifurcations provided the pump parameter is large enough [3]. These papers were focused on the Hopf bifurcations, since for the parameters typical of experimental situations, steady-state bifurcations of the N-mode solution usually take place after Hopf bifurcations. In an attempt to fill this gap, we describe the steady-state bifurcations in a laser with arbitrary total number of modes N. We show that these bifurcations play an important role in the laser dynamics even if they occur after the Hopf bifurcations. In particular, some of them can lead to stable single- or two-mode operation. Thus, the results obtained can be used in order to stabilize the output intensity of a frequency-doubled laser.

II. LASER MODEL

To describe the modal interaction in a frequency-doubled solid-state laser we consider the model proposed in [1]:

$$\eta \frac{dI_k}{dt} = I_k\left(G_k - \alpha + g\epsilon I_k - 2\epsilon \sum_{r=1}^{N} \mu_{kr} I_r \right), \tag{1}$$

$$\frac{dG_k}{dt} = \gamma - G_k\left(1 + (1-\beta) I_k + \beta \sum_{r=1}^{N} I_r \right). \tag{2}$$

I_k (G_k) is the intensity (gain) of the mode k. $\eta = \tau_c/\tau_f$, where τ_c and τ_f are the cavity round-trip and fluorescence lifetime, respectively. α is the cavity loss parameter, β is the cross saturation parameter, and γ is the linear gain parameter. These three parameters are assumed to be the same for all the modes. The total number of laser modes is $N = M + P$, where M and P are the numbers of the modes belonging to orthogonal polarizations. If the modes k and r have the same polarization then $\mu_{kr} = g$ and $\mu_{kr} = 1 - g$ otherwise. The parameter ϵ describes the nonlinear coupling between the modes due to the frequency sum generation in the KTP crystal. For laser parameters typical of experimental situation we have $\epsilon,\ \eta \ll 1$ [1,9–12]. Therefore most analytical results concerning antiphase oscillations in these lasers were obtained in the limit $\epsilon, \eta \to 0$ [3,8,5].

III. STABILITY ANALYSIS

A. N-mode solution

1. $M = P = N/2$

We consider the stability of the steady-state solution for which all modes in a given polarization have nonzero and equal intensities and modal gains. Since for $M \neq P$ explicit expressions for the stability boundaries of the N-mode solution are very cumbersome, we give them only for the case $M = P = N/2 \geqslant 1$. In this case the steady-state solution under consideration is given by

$$I_j = I > 0, \quad G_j = G \quad (j = 1, \ldots, N). \tag{3}$$

The Hopf bifurcation conditions for the solution (3) were derived in [3]. They are given by

$$\gamma=\gamma_{1N}^{H}=\frac{g\epsilon I}{\eta}[\alpha+\epsilon I(N-g)],\quad I=\frac{\eta/\epsilon}{g-(\eta/\epsilon)D_N}>0 \tag{4}$$

and

$$\gamma=\gamma_{2N}^{H}=\frac{\epsilon I}{\eta}D_{1N}[\alpha+\epsilon I(N-g)],\quad I=\frac{\eta/\epsilon}{D_{1N}-(\eta/\epsilon)D_N}>0, \tag{5}$$

where $D_N=1+\beta(N-1)$ and $D_{1N}=N(1-2g)+g$. At the bifurcation boundary (4) the linear stability analysis of the solution (3) yields $N-2$ pairs of pure imaginary eigenvalues, whereas Eq. (5) corresponds to a simple pair of pure imaginary eigenvalues. Hence, for $N>3$ the condition (4) defines a degenerate Hopf bifurcation. This bifurcation produces n periodic solutions where n increases with N. The Hopf bifurcation (5) is nondegenerate for any N and leads to a single time-periodic solution referred to as AD4 in [5,8]: all the modes in each polarization oscillate in phase, while the two polarizations oscillate in antiphase.

Let us introduce the coefficients

$$A=\alpha+g\epsilon,\quad B=\alpha\beta+2g\epsilon,$$

$$A_N=\alpha[1+\beta(N/2-1)]+g\epsilon(N-1),$$

$$B_N=\alpha\beta N/2+N\epsilon(1-g), \tag{6}$$

which describe mode interactions near the linear laser threshold $\gamma=\alpha$. More precisely, the coefficient A (A_N) is the self-saturation coefficient for a solitary mode ($N/2$ identical modes belonging to the same polarization), while B (B_N) is the cross-saturation coefficient for two modes having the same polarization (two groups of $N/2$ modes having different polarizations). $A_2=A$. The coefficients (6) can be easily obtained by adiabatically eliminating the variables G_k in Eq. (2) and expanding the right-hand side of Eq. (1) into powers of the small modal intensities near the lasing threshold. It will be shown later that the stability conditions for steady-state solutions depend on the relations between the saturation and cross-saturation coefficients.

The steady-state (or pitchfork) bifurcations of the solution (3) are defined by

$$\gamma=\gamma_{1N}^{S}=\frac{g(1-\beta)[\alpha D_N+(g-N)\epsilon]^2}{\epsilon[2gD_N-N(1-\beta+g\beta)]^2},$$

$$I=\frac{A-B}{\epsilon[2gD_N-N(1-\beta+g\beta)]}>0, \tag{7}$$

$$\gamma=\gamma_{2N}^{S}=\frac{(1-\beta)D_{1N}[\alpha D_N+(g-N)\epsilon]^2}{\epsilon[N\beta D_{1N}-2g(N-1)(1-\beta)]^2},$$

$$I=\frac{A_N-B_N}{\epsilon[N\beta D_{1N}-2g(N-1)(1-\beta)]}>0, \tag{8}$$

where, according to Eq. (6), we have $A-B=\alpha(1-\beta)-g\epsilon$ and $A_N-B_N=\alpha(1-\beta)-\epsilon D_{1N}$. The condition (7) corresponds to a degenerate bifurcation with $(N-2)$ zero eigenvalues. The number of steady-state solutions bifurcating from the N-mode solution at this degenerate bifurcation increases with N. The condition (8) corresponds to a simple pitchfork bifurcation with a single zero eigenvalue.

Finally, the stability conditions for the solution (3) with $N>2$ are given by

$$\gamma<\gamma_{1N}^{H}\quad\text{or}\quad\eta/\epsilon>g/D_N, \tag{9}$$

$$\gamma<\gamma_{2N}^{H}\quad\text{or}\quad\eta/\epsilon>D_{1N}/D_N, \tag{10}$$

$$\gamma<\gamma_{1N}^{S}\quad\text{or}\quad\beta>\frac{N-2g}{2g(N-1)+N(1-g)}\quad\text{for } A>B,$$

$$\gamma>\gamma_{1N}^{S} \tag{11}$$

and

$$\beta<\frac{N-2g}{2g(N-1)+N(1-g)}\quad\text{for } A<B,$$

$$\gamma<\gamma_{2N}^{S}\text{ or }\beta>\frac{2g(N-1)}{ND_{1N}+2g(N-1)}\quad\text{for } A_N>B_N,$$

$$\gamma>\gamma_{2N}^{S} \tag{12}$$

and

$$\beta<\frac{2g(N-1)}{ND_{1N}+2g(N-1)}\quad\text{for } A_N<B_N.$$

For $N=2$ we only have the two stability conditions (10) and (12).

The Hopf bifurcation surface (9) [(10)] determines the stability of the N-mode solution with respect to a Hopf bifurcation for $g<1/2$ ($g>1/2$). For $\eta/\epsilon<1/(2D_N)$ the two Hopf bifurcation surfaces intersect at $g=1/2$. Otherwise, if $\eta/\epsilon>1/(2D_N)$, there exists an interval of g where a Hopf bifurcation is impossible for any value of the pump parameter γ. This is the case, e.g., when the number of the excited modes N is large enough. In particular, for the parameters of [9] we need $N>25$ in order to suppress the Hopf bifurcation at $g\approx1/2$. For greater values of ϵ and/or smaller values of η, the Hopf bifurcation can be suppressed even in a laser with few modes (see Fig. 3).

Like the Hopf bifurcation boundaries, the steady-state bifurcation surfaces (7) and (8) intersect at $g=1/2$ for $\beta>2(N-1)/(3N-2)$. Note, however, that stable N-mode operation can be observed near the lasing threshold only if the self-saturation coefficients are greater than the cross-saturation coefficients: $A>B$, $A_N>B_N$. This is always true in the limit $\eta,\epsilon\to0$ which corresponds to the experimental situation of [1,9–12].

It follows from Eqs. (4)–(8) that in the limit $\epsilon\to0$, the steady-state (Hopf) bifurcations of Eq. (3) take place for $\gamma=O(1/\epsilon)$ [$\gamma=O(1)$]. Hence, for ϵ small enough, we usually have $\gamma_{1N}^{H}<\gamma_{1N}^{S}$ and $\gamma_{2N}^{H}<\gamma_{2N}^{S}$ and the solutions bifurcating from the N-mode solution at the steady-state bifurcation point are unstable [3]. Nevertheless, even in this case it is worthwhile to study them since they can be involved in the

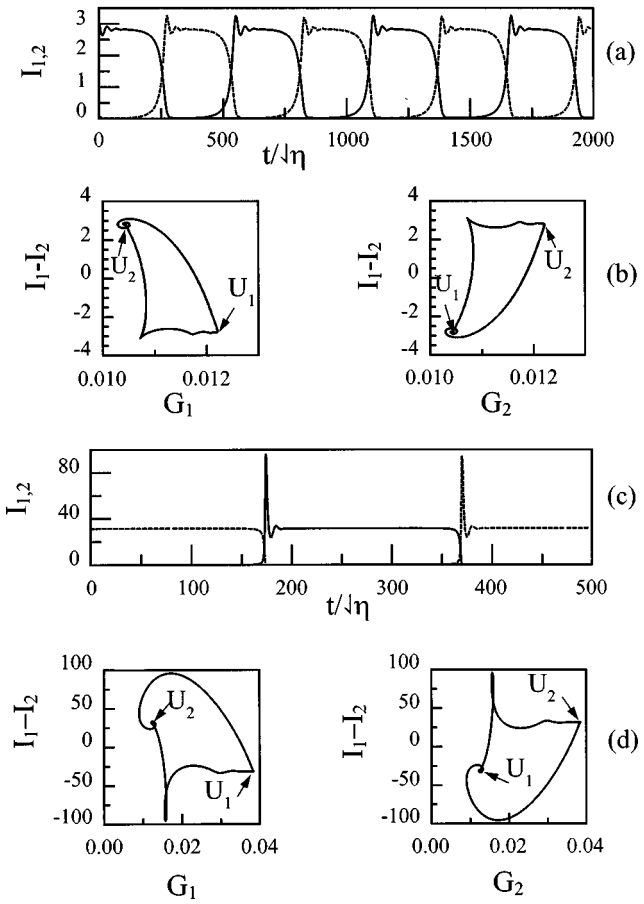

FIG. 1. Time dependence of the modal intensities and phase portraits for a laser with two modes in orthogonal polarizations. The parameters are close to a heteroclininic bifurcation responsible for the breakup of the antiphase oscillations: $\eta=10^{-4}$, $\epsilon=5\times10^{-4}$, $\alpha=10^{-2}$. The points U_1 and U_2 indicate the positions of the unstable single mode steady-state solutions. (a),(b) $g=0.3$, $\gamma=0.04$. (c),(d) $g=0.15$, $\gamma=0.4$.

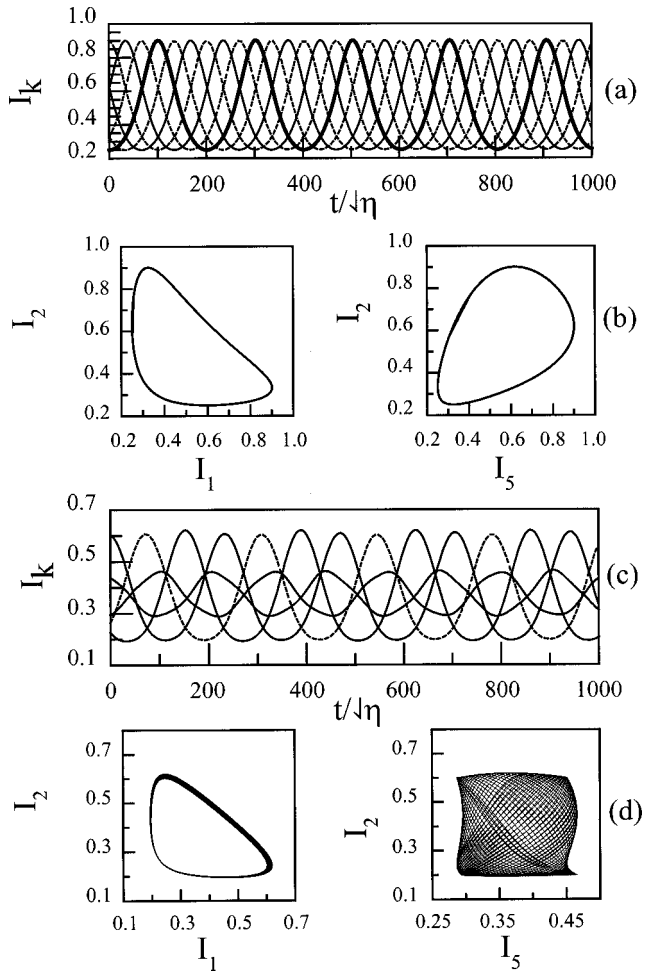

FIG. 2. Antiphase oscillations in a laser with equal and unequal mode numbers in different polarizations with $\eta=10^{-6}$, $\epsilon=10^{-5}$, $\alpha=10^{-2}$, $g=0.7$, $\beta=0.8$. (a) Time evolution of the mode intensities for $L=3$, $P=3$, and $\gamma=0.0335$. (b) Projections of the phase trajectory corresponding to the solutions shown in (a). (c) Time evolution of the modal intensities for $L=3$, $P=2$, and $\gamma=0.0225$. (d) Phase portraits of the solutions shown in (c). The modes 2 and 5 have different polarizations while the modes 1 and 2 belong to the same polarization.

bifurcations leading to stable solutions. Specifically, the pitchfork bifurcation (8) produces two branches of unstable solutions:

$$I_1=\cdots=I_M\equiv I_a,\quad I_{M+1}=\cdots=I_{M+P}\equiv I_b,\quad I_a>I_b, \tag{13}$$

$$I_1=\cdots=I_M\equiv I_a,\quad I_{M+1}=\cdots=I_{M+P}\equiv I_b,\quad I_b>I_a. \tag{14}$$

The difference $|I_a-I_b|$ increases away from the pitchfork bifurcation point (8) and finally the quantity $I_b(I_a)$ drops to zero at the bifurcation point where the solution (13) [the solution (14)] collides with the M-mode (P-mode) steady-state solution for which only one-half of the laser modes belonging to the same polarization have nonzero intensities. After this collision the M-mode (P-mode) solution can become stable.

Bifurcation phenomena associated with the degenerate bifurcation (7) are more complicated. As in the case of nondegenerate pitchfork bifurcation (8), we have unstable steady-state solutions bifurcating from the N-mode solution. Some of these solutions collide with the two-mode solutions, which can become stable after the collision. The other important feature of the unstable solutions bifurcating from the N-mode solution is that under certain conditions they can be involved in homoclinic bifurcations that lead to the transition from antiphase to stable cw operation (see Fig. 1).

2. $M\neq P$

For arbitrary M and P asymptotic expressions for the Hopf bifurcation are given in [8]. Since the expressions for the steady-state bifurcations of the N-mode solution are too complex, even in the limit $\epsilon,\eta\to0$, we do not present them here. However, it is worth discussing qualitative changes that take place when $M\neq P$. It follows from the structure of the characteristic polynomial for the N-mode solution (see [3]) that for $M\neq P$, M, $P>1$ and $M+P>2$, the degenerate Hopf (degenerate pitchfork) bifurcation surface defined by Eq. (4) [Eq. (7)] splits into two separate bifurcation surfaces that correspond to $M-1$ and $P-1$ pairs of pure imaginary eigenvalues (zero eigenvalues), respectively. For η/ϵ

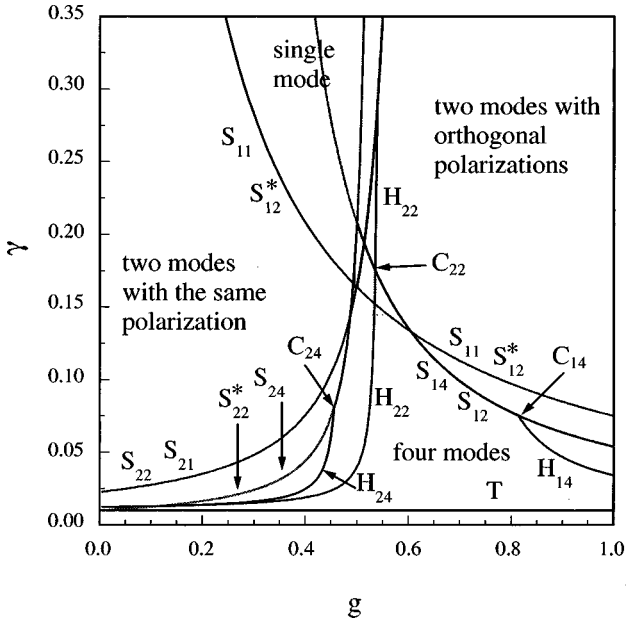

FIG. 3. Bifurcation loci for the steady-state solutions of Eqs. (1) with $L=2$, $P=2$, $\eta=10^{-4}$, $\epsilon=5\times10^{-4}$, $\alpha=10^{-2}$, and $\beta=0.8$. The line T indicates the linear laser threshold $\gamma=\alpha$. The curves S_{1K} and S_{2K} (H_{1K} and H_{2K}) correspond to steady state (Hopf) bifurcations of the K-mode solution with $K/2$ nonzero and equal mode intensities in each polarization. The curves S_{12}^* and S_{22}^* indicate the steady-state bifurcations of the solution for which two modes in one polarization have nonzero and equal intensities. The boundaries of the stability domains are shown by solid lines. Dotted lines correspond to bifurcations of the unstable solutions. Codimension-two points resulting from the interaction of steady state and Hopf bifurcations are labeled C_{14}, C_{24}, and C_{22}.

$<1/(2D_N)$ these surfaces intersect at $g=1/2$. In the case of a Hopf bifurcation, the distance between the two bifurcation surfaces is very small since it is proportional to the small parameter ϵ. Therefore, the two bifurcations take place almost simultaneously. However, even for small ϵ the splitting of the Hopf bifurcation surfaces has an important consequence: the two subsequent Hopf bifurcations correspond to slightly different frequencies. As a result, just after crossing the first Hopf bifurcation surface, a secondary instability leading to quasiperiodic behavior is to be expected. This conclusion is illustrated by Fig. 2, where the time dependence of the modal intensities and phase portraits are shown for Eqs. (1) with $M=P=3$ [Figs. 2(a), 2(b)] and $M=3$, $P=2$ [Figs. 2(c), 2(d)]. The parameters are close to the Hopf bifurcation threshold. It is seen from Fig. 2 that for $M=P$ above the Hopf bifurcation threshold the laser demonstrates the usual AD1 regime [8,5] for which all the modal intensities exhibit identical oscillations with the phase shift T/N between the modes, where T is the oscillation period. By contrast, for $M\neq P$ the modes in different polarizations have unequal amplitudes and frequencies of oscillation. Therefore, in this case we have the quasiperiodic regime [see Fig. 2(d)].

B. Single-mode solution

Let $M\geqslant1$, $P\geqslant0$, and $N=M+P\geqslant2$. Consider the single-mode stationary solution of Eqs. (1):

$$I_1>0, \quad I_j=0 \quad \text{for } j=2,\ldots,M+P. \tag{15}$$

It is easy to check that the solution (15) cannot exhibit a Hopf bifurcation. The stability boundaries for this solution are given by

$$\gamma=\gamma_{11}^S=\frac{(1-\beta)(\alpha-2g\epsilon)(\alpha\beta-g\epsilon)}{g\epsilon(2\beta-1)^2},$$
$$I_1=\frac{A-B}{g\epsilon(2\beta-1)}>0, \tag{16}$$

and

$$\gamma=\gamma_{21}^S=\frac{(2-3g)(1-\beta)[\alpha-(1-g)\epsilon](\alpha\beta-g\epsilon)}{\epsilon[2(1-g)\beta-g]^2},$$
$$I_1=\frac{A-B_2}{\epsilon[2(1-g)\beta-g]}>0, \tag{17}$$

where A, B, and B_2 are the self- and the cross-saturation coefficients defined by Eq. (6) with $N=2$, $A-B=\alpha(1-\beta)-g\epsilon$, $A-B_2=\alpha(1-\beta)-(2-3g)\epsilon$. At the bifurcation boundary Eq. (16) [Eq. (17)] the Jacobian matrix of Eqs. (1) evaluated at the single-mode solution (15) has $M-1$ (P) zero eigenvalues.

For $M>1$ the two stability conditions for the single-mode solution are

$$\gamma>\gamma_{11}^S$$

and

$$\beta>1/2 \quad \text{for } A>B,$$
$$\gamma<\gamma_{11}^S \quad \text{or} \quad \beta>1/2 \quad \text{for } A<B, \tag{18}$$
$$\gamma>\gamma_{21}^S$$

and

$$\beta>\frac{g}{2(1-g)}, \quad \text{for } A>B_2,$$
$$\gamma<\gamma_{21}^S \quad \text{or} \quad \beta>\frac{g}{2(1-g)} \quad \text{for } A<B_2. \tag{19}$$

The first condition (18) describes the stability with respect to small perturbations of the $M-1$ modes having the same polarization as the mode 1. The second condition (19) describes the stability with respect to perturbations of P modes having orthogonal polarization. For $M=1$ ($P=0$) there is only one stability condition (18) [(19)].

For typical experiments, we have $\alpha\gg\epsilon$ and, hence, $A\gg B,B_2$. In this case the single mode solution becomes stable only for sufficiently high pump levels provided the cross-saturation coefficient β is large enough. On the other hand, if the ratio of linear to nonlinear losses α/ϵ is large enough so that the cross-saturation coefficients are smaller than the self-saturation ($A<B$ and $A<B_2$), the laser can start to operate in a single mode just after crossing the linear threshold. In

this case, unlike the case $\alpha \gg \epsilon$, the single-mode operation becomes unstable with increasing of the pump parameter.

The breakup of antiphase oscillations leading to a cw operation was described for a two-mode laser with KTP crystal [1]. A similar transition to a single-mode regime that takes place for sufficiently high gain level and that is referred to as ''breakup of multimode operation'' was very recently observed experimentally in a diode-pumped $LiNdP_4O_{12}$ laser without KTP crystal and studied theoretically [13,14]. It follows from our considerations that one mechanism that could be responsible for the breakup is associated with the nonlinear coupling between the modes due to intensity dependent losses.

C. Two-mode solution

Let $M,P>0$. The steady-state solution with two lasing modes having different polarizations is defined by

$$I_1=I_{M+1}=I>0, \quad I_j=0 \quad \text{for}$$
$$j=2,\ldots,M,M+2,\ldots,M+P. \tag{20}$$

First, let us consider the ''internal'' stability of this solution, i.e., the stability with respect to small perturbations of the two lasing modes, having nonzero intensities at the steady-state solution (20). In other words we study the stability within the invariant manifold $I_j=0$ $(j=2,\ldots,M,M+2,\ldots,M+P)$. The boundaries of this ''internal'' stability domain are defined by Eqs. (5) and (8) with $N=2$:

$$\gamma=\gamma_{22}^H=\frac{\epsilon I}{\eta}(2-3g)[\alpha D_2+\epsilon I(2-g)],$$
$$I=\frac{\eta/\epsilon}{2-3g-(\eta/\epsilon)D_2}>0, \tag{21}$$
$$\gamma=\gamma_{22}^S=\frac{(2-3g)(1-\beta)[\alpha(1+\beta)+(g-2)\epsilon]^2}{4[2(1-g)\beta-g]^2\epsilon},$$
$$I=\frac{A-B_2}{2[2(1-g)\beta-g]\epsilon}>0, \tag{22}$$

with $D_2=1+\beta$. For the case $M+P>2$, apart from this ''internal'' stability conditions, we have to satisfy ''external'' stability conditions which account for the small perturbations of the $M+P-2$ modes having zero intensities at the steady state solution (20). The ''external'' stability boundary for (20) is defined by

$$\gamma=\gamma_{12}^S=\frac{g(1-\beta)[\alpha D_2-2\epsilon][2\alpha\beta+(g-2)\epsilon]}{\epsilon[gD_2-2(1-\beta)]^2},$$
$$I=\frac{A-B}{\epsilon[gD_2-2(1-\beta)]}>0.$$

This boundary corresponds to $M+P-2$ zero eigenvalues of the Jacobian matrix of Eqs. (1).

The stability conditions for the two-mode solution of Eqs. (1) with $N>2$ are defined by

$$\gamma<\gamma_{22}^H \quad \text{or} \quad \frac{\eta}{\epsilon g}>\frac{2-3g}{1+\beta}, \tag{23}$$
$$\gamma>\gamma_{12}^S$$

and

$$\beta>\frac{2-g}{2+g} \quad \text{for } A>B,$$
$$\gamma<\gamma_{12}^S \text{ or } \beta<\frac{2-g}{2+g} \quad \text{for } A<B, \tag{24}$$

$$\gamma<\gamma_{22}^S \quad \text{or } \beta<\frac{g}{2(1-g)} \quad \text{for } A>B_2, \tag{25}$$
$$\gamma>\gamma_{22}^S$$

and

$$\beta>\frac{g}{2(1-g)} \quad \text{for } A<B_2,$$

while for $M=P=1$ we have only ''internal'' stability conditions (25) and (23).

As in the single-mode regime, the stable two-mode solution (20) can be observed only for a sufficiently high pump level if $\alpha \gg \epsilon$. However, it appears for greater values of the parameter g when the cross-saturation between the modes with orthogonal polarizations is weak enough.

D. M-mode solution

Let $M>1,P\geq 0$. Consider the steady-state solution for which all M modes in one polarization have positive and equal intensities, while the remaining P modes with orthogonal polarization have zero intensities

$$I_1=I_2=\cdots=I_M=I>0, \quad I_j=0$$
$$\text{for } j=M+1,\ldots,M+P. \tag{26}$$

As in the case of the two-mode solution, we have both ''internal'' and ''external'' stability conditions. The former (latter) ones describe the stability with respect to small perturbations of nonzero (zero) intensity modes. The ''internal'' stability boundaries for Eq. (26) are obtained by the substitution $N\to M$, $g\to 1/2$, $\epsilon\to 2g\epsilon$ into Eqs. (4)–(8). Since for $g=1/2$ the bifurcation set (4) [(7)] coincides with (5) [(8)], we get only two instability boundaries

$$\gamma=\gamma_{1M}^H=\frac{g\epsilon I}{\eta}[\alpha+g\epsilon I(2M-1)],$$
$$I=\frac{\eta/g\epsilon}{1-(\eta/g\epsilon)D_M}>0, \quad D_M=1+\beta(M-1) \tag{27}$$

and

$$\gamma=\gamma_{1M}^{S}=\frac{(1-\beta)[\alpha D_M-g\epsilon(2M-1)]^2}{g\epsilon[2D_M-M(2-\beta)]^2},$$

$$I=\frac{A-B}{g\epsilon[2D_M-M(2-\beta)]}>0. \tag{28}$$

The coefficients A and B are defined by Eq. (6). The bifurcation set (28) [(27)] is characterized by $M-1$ zero (pairs of pure imaginary) eigenvalues.

The ''external'' stability boundary for the solution (26) corresponds to P zero eigenvalues and is defined by

$$\gamma=\gamma_{2M}^{S}$$

$$=\frac{(1-\beta)D_{1M}[\alpha D_M+2M(g-1)\epsilon][M\alpha\beta-(2M-1)g\epsilon]}{\epsilon[M\beta D_{1M}-g(2M-1)(1-\beta)]^2},$$

$$I=\frac{A_M-B_M}{\epsilon[M\beta D_{1M}-g(2M-1)(1-\beta)]}>0,$$

$$D_{1M}=2M(1-2g)+g,$$

where A_M and B_M are obtained from A_N and B_N in Eq. (6) by the substitution $N\to 2M$. $A_M-B_M=\alpha(1-\beta)-\epsilon D_{1M}$.

Finally, we get the following stability conditions

$$\gamma<\gamma_{1N}^{H} \quad \text{or} \quad \eta/\epsilon>g/D_M, \tag{29}$$

$$\gamma<\gamma_{1M}^{S} \quad \text{or} \quad \beta>\frac{2(M-1)}{3M-1} \quad \text{for } A>B, \qquad \gamma>\gamma_{1M}^{S} \tag{30}$$

and

$$\beta<\frac{2(M-1)}{3M-1} \quad \text{for } A<B,$$

$$\gamma<\gamma_{2M}^{S} \quad \text{or } \beta>\frac{g(2M-1)}{2MD_{1M}+g(M-1)} \quad \text{for } A_M>B_M, \tag{31}$$

$$\gamma>\gamma_{2M}^{S}$$

and

$$\beta<\frac{g(2M-1)}{2MD_{1M}+g(M-1)} \quad \text{for } A_M<B_M,$$

which for $P=0$ are reduced to the ''internal'' stability conditions (29) and (30).

It follows from Eqs. (30) and (31) that the M-mode solution can be stable only if the cross-saturation parameter β is small enough and the nonlinear coupling between the modes with the same polarization is stronger than that between the modes with the same polarization, which implies $g\ll 1/2$. Similarly to the single-mode solution and the two-mode solution in the limit $\alpha\gg\epsilon$, the M-mode solution can be stable only for sufficiently high pump power levels.

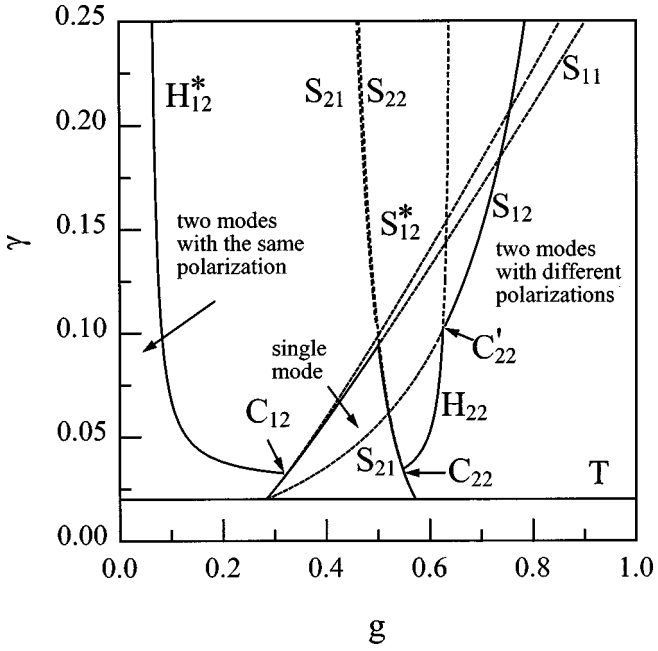

FIG. 4. Bifurcation loci for the steady-state solutions of Eqs. (1) with $L=2$, $P=1$, $\eta=2\times10^{-3}$, $\epsilon=5\times10^{-2}$, $\alpha=2\times10^{-2}$, and $\beta=0.8$. The notations are similar to those in Fig. 3.

E. Other steady-state solutions

In the preceding sections we have studied symmetric steady-state solutions for which modal intensities in a given polarization are equal. We have considered four types of solutions and have shown that for certain parameters any one of them can be stable. All these solutions share the common property that they have 0, 1, or all nonzero mode intensities in a given polarization. Simple considerations show that it is unlikely to find stable ''symmetric'' solutions that cannot be assigned to any of the four types described above (we do not consider here the trivial nonlasing solution). Indeed, since all the modes in Eq. (1) are identical, either none or one mode or all the modes in each polarization can survive in the course of the mode competition. A similar conclusion can be drawn on the basis of linear stability analysis in the limit ϵ, $\eta\to 0$.

When the laser modes have different losses and/or gains the symmetry between the modes belonging to the same polarization is broken. In this case different single-mode solutions should have different stability domains.

IV. BIFURCATION DIAGRAMS

Bifurcation curves for the steady state of solutions of Eqs. (1) are shown in Figs. 3 and 4. Fig. 3 corresponds to a four-mode laser with two pairs of modes in different polarizations. Here the curve H_{14} (H_{24}) denotes a degenerate (simple) Hopf bifurcations of the four-mode solution defined by Eqs. (4) [Eqs. (5)] with $N=4$. The curve S_{14} (S_{24}) defined by Eqs. (7) [Eqs. (8)] corresponds to a degenerate (simple)

pitchfork bifurcation of the four-mode solution. The four-mode solution is stable below the curves S_{14}, S_{24}, H_{14}, and H_{24}. It follows from Fig. 3 that with the increase of the pump parameter depending on the value of the parameter g the four-mode solution can lose stability either via a Hopf or via a pitchfork bifurcation. At the points C_{14} and C_{24} both Hopf and pitchfork bifurcations take place simultaneously and lead to a higher-order degeneracy. When approaching these points along the Hopf bifurcation curve, the imaginary parts of the critical eigenvalues that define the frequency of the emerging periodic solutions tend to zero. Hence, the period of the antiphase oscillations diverges. This clarifies the mechanism of the antiphase oscillation breakup that takes place near the pitchfork bifurcation curve. The period of the pulsed regime arising after the Hopf bifurcation increases with the pump parameter γ. When approaching the pitchfork bifurcation curve, this regime is transformed into a regime similar to that referred as to mode hopping in [15]: the laser exhibits different cw solutions alternating in time. If the pump parameter is further increased the time interval between the hops increases and finally a cw operation becomes stable after a global bifurcation that takes place near the pitchfork bifurcation curve (see Fig. 1). Note that, unlike the case of two-mode laser for which the mode hopping is always periodic, in the case of a laser with more than two modes the mode-hopping regime can be irregular.

The single-mode solution is stable above the curves S_{11} and S_{21} defined by Eqs. (16) and (17), respectively. The stability conditions (18) and (19) do not depend on the total mode number N. Hence, the stability domain of the single-mode solution shown in Fig. 3 is the same for a laser with arbitrary mode number provided that $M=P$ in Eqs. (1) and all the modes in each polarization are identical. It follows from this figure and Eqs. (18), (19) that the single-mode solution can be stable for sufficiently high pump levels ($\gamma \sim \alpha^2/\epsilon$) and only in a definite interval of the parameter g. If the parameter g is small enough, the single-mode regime is unstable. In this case the competition between the two groups of modes having different polarizations is too strong and the laser operates in all modes belonging to a single polarization. By contrast, when the parameter g is large enough the competition between the modes with different polarizations is reduced and for sufficiently high pump levels instead of a single-mode regime the laser demonstrates a regime with two modes having different polarizations. In Fig. 3 the stability domain of the two-mode solution is situated to the left from the curves S_{12}, S_{22}, and H_{22}. The intersection of the steady-state bifurcation curve S_{22} with the Hopf bifurcation curve H_{22} produces the codimension-two point C_{22} that is characterized by a single zero and a pair of pure imaginary eigenvalues. This point is known to be associated with chaotic behavior [16].

Figure 4 presents the bifurcations of the steady-state solutions for a three-mode laser described by Eqs. (1) with $L=2$, $P=1$. The parameters are the same as in [4]. Unlike Fig. 3 for which the linear loss parameter α is much larger than the nonlinear coupling parameter ϵ, here we have $\alpha \approx \epsilon$. As a result, the three-mode solution is unstable just near the linear laser threshold indicated by the line T. Above this line the laser starts to operate either in a single-mode or on two modes. The stability domain of the single mode solution lies below the curves S_{11} and S_{21}. The two-mode solution with modes having orthogonal polarizations (the same polarization) is stable to the right (left) of the curves S_{12}, S_{22}, and H_{22} (S_{12}^* and H_{12}^*). The codimension-two points C_{k2} ($k=1,2$) correspond to the Z_2 symmetric Bogdanov-Takens bifurcations [16,17], which imply the existence of homoclinic bifurcations. The global bifurcations responsible for the breakup of the antiphase oscillations are similar to those in described for a bidirectional class B laser [18]. The codimension-two point C_{22} in Fig. 4 corresponds a simple zero and a pair of pure imaginary eigenvalues and is similar to that shown in Fig. 3. Chaotic solutions associated with this point were observed in numerical calculations of [4].

V. CONCLUSION

We have studied the bifurcations of the steady-state solutions in an intracavity frequency-doubled solid-state laser and have shown that for sufficiently large gains a breakup of multimode operation can take place, leading to a stable single-mode or two-mode regime. For the laser parameters typical of experimental situations, the N-mode solution is known to be stable only for rather low pump levels. With an increase of the pump parameter, it undergoes a Hopf bifurcation leading to antiphased regimes characterized by large-amplitude fluctuations of the output intensity. If the pump parameter is further increased, the period of the antiphase pulsations grows and the so-called mode hopping takes place. In the course of the mode hopping, the laser demonstrates switching between different cw solutions. Finally, for sufficiently strong pumping, the period of the antiphase pulsations diverges and a transition takes place to a cw regime corresponding to a single- or a two-mode solution. Bifurcation mechanisms of the multimode antiphase pulsation breakup are associated with global bifurcations involving homoclinic connections. Here we have performed a detailed study of the bifurcations of the steady-state solutions of Eqs. (1) and derived analytical conditions for the multimode operation breakup. We have shown that a stable cw operation is possible in a frequency-doubled laser in the high gain domain provided the cavity losses are small enough. More precisely, it follows from Eqs. (18), (19) that in order for the single mode solution to be stable in a certain interval of g, the inequality $\gamma > \alpha^2 2\beta(1-\beta)/\epsilon(2\beta-1)^2$ has to be satisfied. In particular, for the parameters of [9] ($\alpha=0.01$, $\beta=0.6$, $\epsilon=5\times10^{-5}$) we get the condition $\gamma>24$ for the existence of the stable single-mode solution. For smaller values of α and/or greater ϵ, the single-mode operation can appear at lower gain levels. Note that, as a rule, the regimes that appear at high gain levels have smaller nonlinear losses in the KTP crystal than the N-mode regime which is stable for small values of the pump parameter.

The transition to a single-mode operation in a two-mode frequency-doubled laser was observed experimentally [1]. Similar phenomena were observed in a multimode solid-state laser even without a frequency-doubling crystal [13]. The number of oscillating modes decreased with the increase of the pump parameter and for sufficiently high gain levels a laser demonstrated a single-mode operation. Although the

nonlinear losses due to sum frequency generation in the KTP crystal that are responsible for the breakup of the multimode regime in a frequency-doubled laser were missing in the experiment described in [13] it seems likely that some other kind of nonlinear losses took place there. Here we have shown that intensity-dependent losses can result in the transition from multimode to single-mode operation.

ACKNOWLEDGMENTS

This research was supported by the Fonds National de la Recherche Scientifique, the Interuniversity Attraction Pole program of the Belgian government, a grant from the Services Fédéraux des Affaires Scientifiques, Techniques et Culturelles and an INTAS grant.

[1] T. Baer, J. Opt. Soc. Am. B **3**, 1175 (1986).
[2] P. Mandel, *Theoretical Problems in Cavity Nonlinear Optics* (Cambridge University Press, Cambridge, 1997).
[3] J.-Y. Wang and P. Mandel, Phys. Rev. A **48**, 671 (1993).
[4] P. Mandel and J. Wang, Opt. Lett. **19**, 533 (1994).
[5] J.-Y. Wang and P. Mandel, Phys. Rev. A **52**, 1474 (1995).
[6] E. A. Viktorov and P. Mandel, Opt. Lett. **22**, 1568 (1997).
[7] X.-G. Wu and P. Mandel, J. Opt. Soc. Am. B **4**, 1870 (1987).
[8] J.-Y. Wang, P. Mandel, and T. Erneux, Quantum Semiclassic. Opt. **7**, 169 (1994).
[9] C. Bracikowski and R. Roy, Chaos **1**, 49 (1991).
[10] N.B. Abraham, L.L. Everett, C. Iwata, and M.B. Janiki, Proc. SPIE **2029**, 16 (1993).
[11] E.A. Viktorov, D.R. Klemer, and M.A. Karim, Opt. Commun. **113**, 441 (1995).
[12] V.I. Ustyugov, O.A. Orlov, M.M. Khaleev, G.E. Novikov, E.A. Viktorov, and P. Mandel, Appl. Phys. Lett. **71**, 154 (1997).
[13] K. Otsuka, R. Kawai, Y. Asakawa, P. Mandel, and E.A. Viktorov, Opt. Lett. **23**, 201 (1998).
[14] K. Otsuka, P. Mandel, and E.A. Viktorov, Phys. Rev. A **56**, 3226 (1997).
[15] H. Hennequin, D. Dangoisse, and P. Glorieux, Opt. Commun. **79**, 200 (1990).
[16] J. Guckenheimer and P. Holmes, *Nonlinear Oscillations, Dynamical Systems and Bifurcations of Vector Fields* (Springer, Heidelberg, 1983).
[17] V.I. Arnold, *Geometrical Methods in the Theory of Ordinary Differential Equations* (Springer, Heidelberg, 1983).
[18] A.G. Vladimirov, Opt. Commun. **149**, 67 (1998).